High-Resolution Profiling of the Polyimide−Polyimide Interface

Nancy C. Stoffel,* Chi-An Dai, and Edward J. Kramer*

Department of Materials Science and Engineering, Cornell University, Ithaca, New York 14853

Thomas P. Russell, Vaughn Deline, and Willi Volksen

IBM Almaden Research Center, 650 Harry Road, San Jose, California 45120

Wen-li Wu and Sushil Satija

National Institute of Standards and Technology, Gaithersburg, Maryland 20899

Received February 6, 1996[⊗]

ABSTRACT: Dynamic secondary ion mass spectrometry (SIMS), nuclear reaction analysis, and neutron reflectometry were used to profile polyimide−polyimide interfaces. For interfaces between two layers of poly(4,4′-oxydiphenylene−pyromellitimide) (PMDA−ODA) polyimide it was determined that the interfacial fracture energy G_c and the interfacial width depended primarily upon the imide fraction, f, of the base layer. For $f < 0.9$, there was a sharp interface between the deuterium-labeled poly(amic acid ethyl ester) (dPAE) and the base layer with a long low volume fraction tail of dPAE penetrating into the base layer. The volume fraction of the penetrant was limited by the imide fraction of the base layer and approached zero for $f > 0.9$. The PMDA−ODA/PMDA−ODA interface formed with a fully imidized base layer was ∼30 Å in width, whereas that formed when $f = 0.9$ was ∼80 Å in width. The interface formed during the spin-casting process did not broaden significantly after annealing at 400 °C. We also investigated the interface between a more flexible thermoplastic polyimide poly(4,4′-oxydiphenylene−oxydiphthalimide) (ODPA−ODA) and a fully imidized PMDA−ODA layer. The shape of the ODPA−ODA/PMDA−ODA interface was found to depend upon annealing temperature. Unannealed samples and samples annealed at 350 °C could be fit with an error function, and the interfacial width was ∼50 Å. Samples annealed at 400 and 450 °C were best fit by a fairly sharp interfacial profile with ODPA−ODA tails proceeding into the PMDA−ODA layer. The volume fraction of the ODPA−ODA in the PMDA−ODA depended upon the annealing temperature T_{ann}. The G_c of the ODPA−ODA/PMDA−ODA interface appears limited by the solubility of ODPA−ODA in PMDA−ODA.

Introduction

Multilayer polyimide films are used as interlayer dielectrics on semiconductor chips or multichip modules, as carrier films for tape automated bonded structures (TAB), and for flexible interconnects. Typically, the polyimide derived from pyromellitic dianhydride and 4,4′-oxydianiline is used and is denoted as PMDA−ODA. This polyimide is insoluble in most solvents. Consequently, a solution of a precursor polymer, either the corresponding poly(amic acid) or a poly(amic acid alkyl ester), is cast onto the surface and treated at an elevated temperature to convert the precursor into a polyimide. The fraction of amic acid or amic acid ethyl ester moieties which are transformed into the five-member imide ring is denoted as the imide fraction f. In preparing a multilayered structure, therefore, the interface formed between the precursor polyimide layer and the underlying layer is of importance since this will dictate the adhesion of successive layers. Herein, this interface between two layers of PMDA−ODA was examined using ion beam and neutron reflection techniques.

In this study the relationship between the interfacial fracture energy and the interfacial profiles for PMDA−4,4′-ODA polyimide is examined using high-resolution techniques to profile the interfaces. The imide fraction of the base layer was varied from $0.5 < f < 1$, and its effect upon the penetration of the second layer was measured. The relative contributions of thermal and solvent-enhanced diffusion were ascertained by analyzing the samples after deposition of the second layer, and after the bilayer sample has been annealed at 400 °C for 1 h. These measurements of interfacial width were correlated with measurements of the interfacial fracture energy G_c.

In our previous work[1] the interdiffusion of polyimide layers was examined with forward recoil spectrometry (FRES). It was determined that this technique does not have sufficient resolution to probe the narrow interfaces formed when a polyimide precursor is deposited upon a base layer with imide fraction >0.7. For this reason a variety of higher resolution depth profiling techniques were utilized, including nuclear reaction analysis (NRA), dynamic secondary ion mass spectrometry (DSIMS), and neutron reflectometry (NR). It was important to use a combination of techniques due to their differing resolutions and sensitivities. FRES, DSIMS, and NRA have the advantage of providing composition profiles in real space. While NR probes the composition profiles in momentum space, the spatial resolution of NR is far superior to that of the ion beam techniques. However, the knowledge gained from the ion beam techniques can be invaluable in quantitatively determining concentration profiles from NR data. It should also be noted that NR is insensitive to shallow gradients in concentration which can be easily profiled with the ion beam techniques, further emphasizing the complementary nature of the techniques.

Recently, several methods have been developed to increase the self-adhesion of polyimides when it is not practical to use a partially imidized base layer. One method of adhesion enhancement involves swelling the fully imidized base layer with solvent before deposition

[⊗] Abstract published in *Advance ACS Abstracts,* August 1, 1996.

S0024-9297(96)00188-X CCC: $12.00

and imidization of the second layer.[2,3] DSIMS and neutron reflectivity were used to profile interfaces formed by first solvent swelling the base layer in an effort to determine the mechanism of adhesion enhancement.

In another work, we describe efforts to utilize the thermoplastic polyimide poly(4,4′-oxydiphenylene−oxydiphthalimide) (ODPA−ODA) (with a glass transition temperature of 270 °C) as an adhesive interlayer between two spun-cast PMDA−ODA layers.[4] The weakest interface in these structures was the interface between the fully imidized PMDA−ODA layer and the ODPA−ODA. In this study we also determined the segment density profile of the PMDA−ODA/ODPA−ODA interface as a function of the annealing temperature, and of the molecular weight of the ODPA−ODA using the high-resolution depth profiling techniques.

Experimental Section

Materials. In the diffusion studies of PMDA−ODA, the meta-isomer of the poly(amic acid ethyl ester) precursor (*m*-PAE) was used. The layers were spun cast onto a flat substrate, and the concentration gradients normal to the interface were measured. Contrast between the two layers was provided through labeling the 4,4′-oxydianiline moiety with deuterium. The polymer denoted *m*-dPAE had a $M_w \sim 40\,000$. The synthetic procedure is described in several publications.[5,6]

The poly(amic acid) of ODPA−ODA was synthesized using standard techniques[7] from highly purified dry monomers: 4,4′-oxydianiline (ODA) and 3,3′,4,4′-oxydiphthalic anhydride (ODPA). Three different molecular weight polymers were prepared by varying the stoichiometric imbalance of dianhydride to diamine from 0.965 to 0.985 to 0.995 to obtain predicted molecular weight values of 27 000, 64 000, and 190 000.

Analysis of Interfacial Width. In all of the samples prepared for analysis the interface between the two polymer layers is narrow relative to the thickness of these layers. Both deuterium-labeled and protonated layers are semi-infinite. Therefore the solution of Fick's second law, assuming a concentration independent diffusion coefficient, is

$$C(z) = C_o \operatorname{erfc} \frac{z}{\sqrt{4Dt}} \tag{1}$$

where C_o is the concentration at the interface, D is the time-averaged diffusion coefficient, $w = \sqrt{4Dt}$ is the interdiffusion distance, $d = \sqrt{2\pi}w$ is the width of the interface, and z is the distance from the interface. Initial attempts were made to fit the interfaces using a profile with this shape for all of the experiments described in this paper. This was done with varying degrees of success. In many cases, however, sharp interfaces with long low-concentration tails were observed which could not be fit by the Fickian result, as described in the results section.

Nuclear Reaction Analysis. A 1.7 MV Tandetron accelerator was used to accelerate ^{3}He ions onto the sample at a glancing angle. The impact of ^{3}He onto deuterons results in a nuclear reaction and the formation of an unstable ^{5}Li nucleus. This nucleus decays and the net reaction is as shown below.

$$^3\mathrm{He} + {}^2\mathrm{H} \rightarrow {}^4\mathrm{He} + {}^1\mathrm{H} + Q \qquad \text{where } Q = 18.352 \text{ MeV}$$

The resolution of the NRA technique (~200 Å) is much improved over that of FRES due to an energy amplification effect.[8] Small differences in the energy of the incoming ^{3}He caused by inelastic collisions in the polymer layer will produce large differences in the energy of the forward recoiling ^{4}He. NRA also differs from FRES in that there is no overlap between the hydrogen and deuterium signals, as NRA is only sensitive to the deuterium depth profile.

Samples were prepared by spin casting a 2−3 μm base layer of unlabeled *m*-PAE onto a silicon wafer and drying at 80 °C. The samples were heated to an imidization temperature, T_i, in a nitrogen-purged tube furnace and held at this temperature for 1 h. Subsequently, a layer of the deuterium-labeled poly(amic acid) precursor of PMDA−ODA (dPAA) ~800 Å thick was spin coated onto the base layer and the bilayer sample was annealed at 400 °C.

DSIMS. DSIMS samples were prepared on 1 in. polished quartz disks. The *m*-PAE precursor of the PMDA−ODA-based polyimide was spun cast onto the quartz disks and subsequently dried on a hot plate at 80 °C and thermally imidized. A nitrogen-purged tube furnace was used to heat samples to the imidization temperature T_i and hold them at this temperature for 1 h. A second layer of the deuterium-labeled *meta*-poly(amic acid ethyl ester) of PMDA−ODA was either spun cast onto the base layer or floated on from the surface of a water bath. The bilayer samples were then heated to 400 °C in order to fully imidize the two layers. This procedure ensures that the sputter rate of the ion beam in the two layers is the same during the DSIMS profiling.

The samples were analyzed with a Perkin-Elmer 6300 secondary ion mass spectrometer. The primary ion beam species was O_2^+ supplied at an energy of 2 keV, and the primary ion beam current was 10 nA. The ion beam was rastered to create a crater of ~550 μm × 550 μm. Secondary ions were collected from a 165 μm × 165 μm region in the center of the sputtered crater. The number of secondary ions detected in the mass spectrometer was determined as a function of time. The time scale was converted to a depth scale using the sputtering rate of 3.17 Å/s determined for the PMDA−ODA polyimide. The instrumental resolution was ~160 Å.

Neutron Reflectometry. The technique of neutron reflection is capable of providing information about buried interfaces on a much finer scale than any other depth profiling technique available. Information about sharp jumps in the composition profiles perpendicular to the reflecting surface can be deduced with subnanometer resolution. This technique operates on principles analogous to optical reflection. Snell's law, defining a critical, θ_c, angle below which neutrons do not penetrate the interface, is given by

$$n_0 \cos \theta_0 = n_i \cos \theta_i$$

where n_i is the neutron refractive index in medium i, θ_0 is the grazing angle of incidence, and θ_i is the angle of refraction. If we consider the air/specimen interface, $n_0 = 1$, and n is defined as $n = 1 - \lambda^2/2\pi(b/V)$, where b/V is the neutron scattering length density of the material. Values of the refractive index are generally close to but less than 1 where $1 - n \sim 10^{-6}$. Hence $\theta_i < \theta_0$ and we can define a critical angle θ_c given by $\theta_c/\lambda = (b/\pi V)^{1/2}$ below which neutrons are totally externally reflected at the surface.

The z-component of the neutron momentum in vacuum, $k_{z,0}$, is defined in terms of λ and θ as $k_{z,0} = (2\pi/\lambda) \sin \theta$. The neutron momentum within a medium is reduced by an amount related to the scattering length density of the medium and can be written in terms of the critical neutron momentum, $k_{c,}i$, as

$$k_{z,i} = (k_{z,0}{}^2 - k_{c,i}{}^2)^{1/2}$$

where

$$k_{c,i} = (2\pi/\lambda) \sin \theta_c = (4\pi(b/V)_i)^{1/2}$$

Thus, when $k_{z,i} < k_{c,i}$ the neutrons are totally externally reflected. The reflection coefficient at the air (vacuum)/sample interface, $r_{0,i}$, is defined by

$$r_{0,i} = \frac{k_{z,0} - k_{z,i}}{k_{z,0} + k_{z,i}}$$

Consequently, for a sharp interface, the Fresnel reflectivity is defined by

$$R_f = r_{0,i} r^*_{0,i} = \left| \frac{k_{z,0} - k_{z,i}}{k_{z,0} + k_{z,i}} \right|^2$$

It should be noted that the reflection coefficients can be complex if the medium is absorbing or if, as in the case of neutrons within a hydrogenated medium, there is a substantial amount of incoherent scattering. If we examine R_f at large $k_{z,i}$, it can easily be shown that $R_f \propto k_{z,i}^{-4}$. However, if the interface is rough and we can define a root mean square roughness of σ, then the reflectivity, R, is given in terms of R_f as

$$R = R_f e^{-4k_{z,i}\sigma^2}$$

This equation shows that R is exceptionally sensitive to small amounts of interfacial roughness, i.e. where the gradient in the scattering length density is large. However, if the gradient in scattering length density is small or if σ is too large, then reflectivity becomes insensitive.[9]

Neutron reflectometry has emerged as an important tool for the investigation of polymer interfaces. There can be significant difference in scattering lengths between nuclei that only differ by one nucleon, i.e. isotopes. For example, hydrogen and deuterium have scattering lengths of -0.372×10^{-12} and 0.67×10^{-12} cm, respectively.[10] The isotopic substitution of deuterium for protons provides an easy means of producing contrast between different molecules on a chain. The substitution also produces only a minor perturbation in the thermodynamics which is of only secondary importance.

Experiments were carried out at both the Intense Pulsed Neutron Source at Argonne National Laboratory (IPNS-ANL) in Argonne, IL, and the National Institute of Standards and Technology (NIST) in Gaithersburg, MD. IPNS-ANL has a spallation source and hence neutrons are provided in a range of wavelengths from 3 to 14 Å.[11] In order to cover a large range in k space, three different incident angles were used. NIST has a reactor source so the neutron beam is monochromated to a fixed wavelength and the incident angle is varied in order to vary k.

Data from NR were fit by assuming a scattering length density profile, calculating the reflectivity as a function of k, and comparing the calculated R with the experimental R. A measurement of the closeness of the match between the experimental data and the simulation (χ^2) was calculated, and this value was minimized. The experiments were calibrated by use of a standard that was a deuterated polystyrene film of known thickness on silicon. This provided an easy and convenient means of determining the instrumental resolution and checking the analysis procedures. Each time a group of samples was run, we ran a standard sample which consisted of a layer of deuterated polystyrene on silicon.

Samples for neutron reflection were prepared on either 5 or 10 cm diameter polished silicon wafers, ~5 mm thick. Before use, the silicon wafers were cleaned to remove organic contaminants using a two-step process; first, wet etching in Nanostrip solution from Cyantek, and then dry etching in an oxygen plasma. A layer of the *m*-dPAE was spun cast onto the wafer. The film was then dried on a hot plate at 80 °C, heated in a nitrogen-purged oven at 3 °C/min to the imidization temperature T_i, held for 1 h, and then cooled at ~3 °C/min to room temperature. Next, a layer of unlabeled polymer, either the *m*-PAE precursor of PMDA−ODA or the poly(amic acid) precursor of ODPA−ODA, was spun cast onto the first layer and dried on a hot plate at 80 °C. Some of the samples were analyzed with neutron reflectometry at this point to determine the width of the interface before subsequent annealing. The bilayer samples were annealed in a nitrogen-purged oven at the annealing temperature T_{ann} for 1 h. In all cases, one of the two layers was ~1400−2500 Å thick and the other was 300−800 Å thick. In this way the oscillations in the data that arise from interference will have different periods.

We chose to use the deuterium-labeled polymer on the bottom layer and the protonated layer as the top layer in order to make bilayer polyimide samples with the best sensitivity to changes in interfacial width when analyzed both before and after annealing at 400 °C. The atomic composition and the density are altered as the PAE converts to polyimide, and as f increases the b/V of the polymer layer will increase. The limit of Rk^4 as $k \rightarrow \infty$ depends upon the sum of the squares of the differences in b/V at the interfaces. The amplitude of the oscillations corresponding to the thickness of the polymer layers will also be determined by $\Delta(b/V)$ at the polymer−polymer interface. Since the damping of these oscillations is used in order to determine the width of the polymer−polymer interface, we wanted to maximize $\Delta(b/V)$ at the polymer−polymer interface. Figure 1 shows simulated reflectivity data plotted as Rk^4 vs k for samples constructed with deuterium-labeled top layers and unlabeled bottom layers and vice versa. Simulated data are shown for samples examined both after the 750 Å thick second layer was spun cast ($f = 0$) onto the 2000 Å base layer and after it was imidized ($f = 1$), with a corresponding decrease in top layer film thickness to 500 Å. Parts a and b of Figure 1 show that the size of the oscillations is maximized for the pre-anneal samples through our chosen configuration of use of a top layer of unlabeled PAE and a bottom layer of d-PAE. In Figure 1a $\Delta(b/V) = 0.5 \times 10^{-6}$ Å^{-2}, while for Figure 1b $\Delta(b/V) = 2.8 \times 10^{-6}$ Å^{-2}. The damping of the oscillations gives information about the interfacial width, and hence it is important that they have a fairly large amplitude so that changes in the amplitude of the oscillations are obvious. For samples which have been fully imidized, the value of $\Delta(b/V)$ is the same regardless of the layer order. In this case, as shown in Figure 1c,d, there is little difference between the simulated profiles.

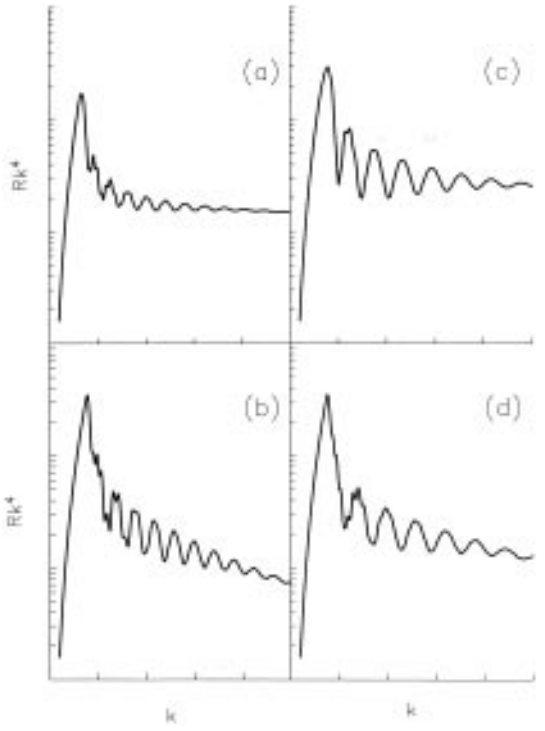

Figure 1. Simulated reflectivity profiles for bilayers of PMDA−ODA plotted as Rk^4 vs k: (a) unlabeled fully imidized base layer and a top layer of dPAE after spin casting; (b) deuterium-labeled fully imidized base layer and a top layer of PAE after spin casting; (c) unlabeled fully imidized base layer and a top layer of dPAE after a 400 °C anneal; (d) base layer of deuterium-labeled fully imidized base layer and a top layer of PAE after a 400 °C anneal.

Measurements of G_c. *T*-peel tests were used to provide a measure of the strength of the polyimide−polyimide interface. Samples were prepared using Ciba-Geigy's Probimide 9767 which is the meta-isomer of the poly(amic acid ethyl ester) precursor of PMDA−ODA. A base layer was spun cast onto 4 in. square glass plates and heated in a nitrogen-purged oven to T_i. All samples were ramped to 150 °C at 1.5 °C/min and then ramped to T_i at 3 °C/min and held at T_i for 1 h before cooling to room temperature. A strip of gold, 1 cm in width

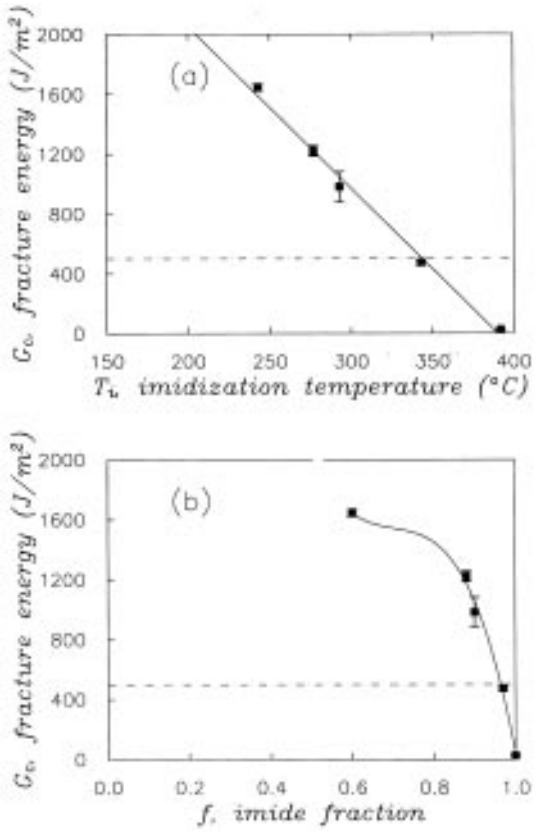

Figure 2. G_c as function of (a) base layer imidization temperature and (b) as a function of base layer imide fraction.

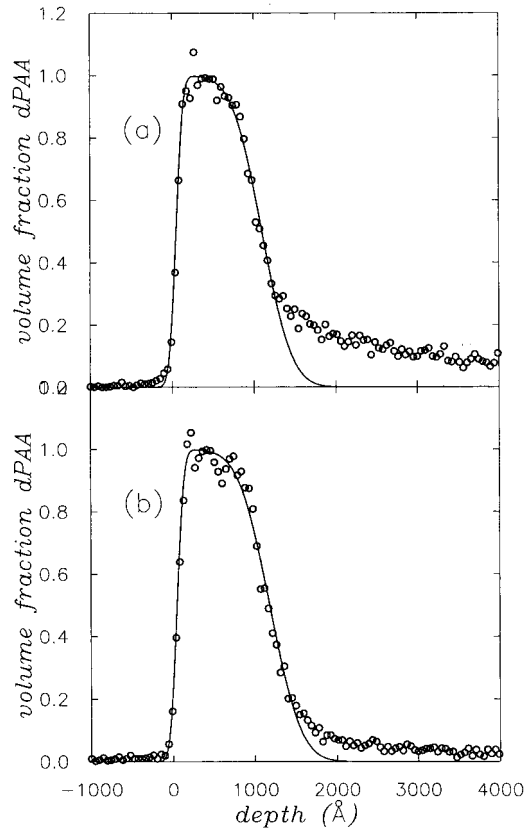

Figure 3. Nuclear reaction analysis data converted into deuterium profiles of PMDA−ODA interfaces: (a) T_i = 240 °C; (b) T_i = 270 °C.

and ∼600 Å thick, was evaporated at one end of the base layer to initiate the crack. The second layer was spun cast onto the first, and the bilayer was heated to 400 °C as described above. Each layer was approximately 25 μm thick. The films were removed from the glass and cut into 7 mm strips. An Instron testing machine was used to perform the *T*-peel tests using a rate of 0.5 in./min. At least six strips were peeled per sample.

It is well-known that the measured G_c from a *T*-peel test will depend upon the mechanical properties of the peel strips since much of the measured energy goes into plastic bending and deformation of the strip rather than into creating a new interface. In order to be able to compare the G_c values obtained for the PMDA−ODA/ODPA−ODA interfaces with the PMDA−ODA/PMDA−ODA interfaces we had to minimize the effect of the ODPA−ODA on the mechanical properties of the peel strips. We prepared samples for testing of the PMDA−ODA/ODPA−ODA interface with a 25 μm base layer of PMDA−ODA, a 2000 Å layer of ODPA−ODA, and a 25 μm top layer of PMDA−ODA. As a result it should be reasonable to compare the G_c values obtained for the PMDA−ODA/PMDA−ODA interfaces with those for the PMDA−ODA/ODPA−ODA interfaces.

Results and Discussion

Interfaces of PMDA−4,4′-ODA/PMDA−4,4′-ODA. Figure 2a shows the relationship between interfacial fracture energy G_c and base layer imidization temperature T_i. Figure 2b shows the relationship between G_c and base layer imide fraction *f*. In these figures it is apparent that G_c decreases as T_i and *f* increase. There is an inverse relationship between the imide fraction of the base layer and the amount of interdiffusion measured with FRES.[1] Hence these data for G_c are consistent with the hypothesis that G_c is strongly correlated to the width of the interface. The G_c that results when a layer is spun cast onto a fully imidized base layer (f = 1) is ∼30 J/m². The G_c value increases dramatically with only a small decrease in the base layer imide fraction. The interface is too strong to measure when f < 0.6 because the arms of the sample tear off.

For 0.6 < f < 1.0 the interfacial widths are too narrow to be resolved with FRES. However, quantitatively characterizing these interfaces over this *f* range is critical, since G_c dramatically changes from being poor to acceptable to excellent. (According to some sources in the electronics industry, an acceptable value of G_c, measured with this form of peel test is ∼500 J/m².[12] Interfaces with G_c > 1000 J/m² are considered excellent.[13])

Bilayer samples made with different imide fraction base layers were examined with NRA. Figure 3 shows the deuterium profiles of bilayer samples with (a) T_i = 240 °C and (b) T_i = 265 °C where the surface of the dPAA is at depth 0 and the interface between the spun-on dPAA layer and the unlabeled base layer is ∼1200 Å below the surface. The solid line in these figures corresponds to a fit obtained using eq 1, an erfc function, the functional form predicted by the solution of Fick's second law for a system with a diffusion coefficient independent of concentration. Obviously, the Fickian profile is not a good fit to the data. These profiles show rather dramatically that the compositional profile is not symmetric; instead, there is a rather sharp interface between the layers with a low volume fraction tail corresponding to a penetration of the dPAA species several thousand angstroms into the base layer. One contribution to the deviation from Fickian behavior is the differences in mobility between the spun-on dPAA and the base layer. The diffusivity of the d-PAA chains into the base layer will be very different from the diffusivity of the base layer into the dPAE. Since the imide fraction of the base layer is greater than 0.5 for

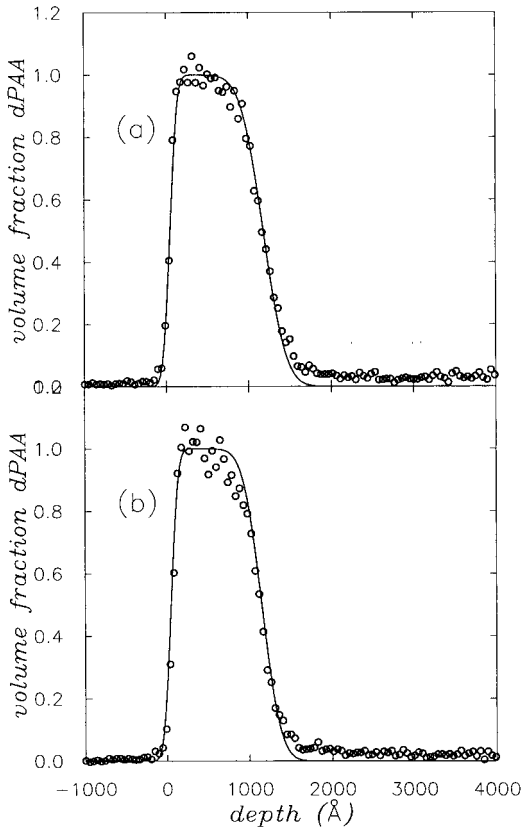

Figure 4. Nuclear reaction analysis data converted into deuterium profiles of PMDA−ODA interfaces: (a) T_i = 300 °C; (b) T_i = 400 °C.

both samples in Figure 3, the T_g of the base layer will be higher than room temperature, and the material is glassy. During the spin-casting process the solvent will plasticize the material and increase the mobility of the chains to some degree. However, it is apparent from the profiles in Figure 3 that the bulk of the diffusion across the interface corresponds to dPAA chains moving into the base layer.

Figure 4 shows the deuterium profiles from NRA that correspond to T_i = 300 °C and T_i = 400 °C base layer samples. These profiles differ from the samples prepared with lower imide fraction base layers in that the interface between the protonated and the deuterated layer can be fit fairly well by a Fickian profile. The volume fraction of the tail has been essentially eliminated. While these profiles are virtually identical, the G_c values of *T*-peel samples where T_i = 300 °C and T_i = 400 °C differ by more than 1 order of magnitude. Consequently, higher resolution techniques are required to differentiate between interfaces prepared with f > 0.9.

DSIMS has slightly better resolution than NRA and was also used to profile the interfaces that resulted from spin casting *m*-PAE onto base layers with various imide fractions. Figure 5 shows deuterium profiles obtained with DSIMS for various base layer imide fraction samples. Again we see that the deuterium concentration profiles are not symmetric. With the improved resolution we can ascertain that there is a rather sharp interface between the layers, which broadens slightly as f decreases, and a long low volume fraction tail of deuterium penetrating the base layer. This result suggests that there is partial solubility of the dPAE chains in the base layer and that the solubility depends upon the imide fraction of the base layer.

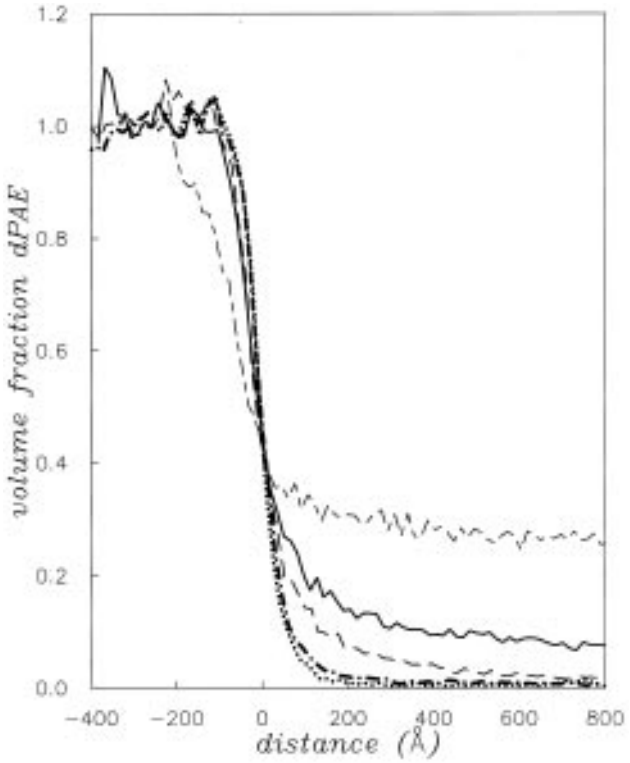

Figure 5. Deuterium depth profiles of isotopically labeled PMDA−ODA interfaces as determined with DSIMS. (− - −) T_i = 250 °C; (—) T_i = 265 °C; (− − −) T_i = 290 °C; (−·−) T_i = 300 °C; (···) T_i = 400 °C.

The profiles of samples with T_i = 300, 350, and 400 °C (0.9 < f < 1) appear indistinguishable and demonstrate that there is no significant penetration of the deuterium-labeled polyimide into the base layer. The width of the interfaces measured with DSIMS is ∼170 Å, essentially the resolution of the technique. It seems likely that the interfacial width may be considerably sharper than the values measured with DSIMS, primarily because there are significant differences in G_c for samples with 0.9 < f < 1 despite the fact that their interfacial widths appear identical. Thus while the DSIMS has provided more detail than FRES about the interfaces, we need a still higher resolution technique to resolve the differences at very high f.

The DSIMS samples differed from those in the NRA experiments in that the top layer was dPAE, but the results were very similar to the NRA experiment where a dPAA top layer was spun on. The similarity in the profile shapes for the two polyimide precursors is consistent with earlier observations that small differences in the structure of the spun-on tracer layer (including variations in the leaving group or isomeric structure of the polyimide precursor) do not result in measurable differences in the interpenetration behavior.[1]

The bulk of the interdiffusion between the polyimide precursor, dPAA or dPAE, and the PI occurs during the spin-casting/drying process. Using FRES, Tead et al.[14] showed that the diffusion process is facilitated by the presence of solvent. The higher resolution capabilities of DSIMS were used to determine if any thermally activated diffusion occurred between the isotopically labeled polyimide layers at elevated temperatures. A bilayer sample was prepared without solvent swelling of the base layer by spin casting a dPAE film on glass, then floating it off onto the surface of a water bath, and transferring this film to a base layer with f = 0.9. The

samples were examined before and after a 400 °C anneal for 1 h. The deuterium and hydrogen profiles were well fit using an error function. The width of the interface both before and after the anneal was 175 Å. Since the interfacial width was unchanged by the annealing process, one can conclude that any thermal diffusion between the layers was much less than 175 Å. These results are not unexpected given the extremely high glass transition temperature of the fully imidized PMDA−ODA base layer.

The asymmetry of the NRA and DSIMS profiles suggests that the PAE has sufficient mobility to penetrate the base layer, but the base layer polyimide is prevented from diffusing into the PAE layer by the stiffness of the chains. However, there is sufficient mobility for it to be swollen by the PAE chains. Figures 3 and 5 show that the volume fraction of PAE chains that penetrate the base layer depends upon the imide fraction of the base layer. As the imidization of the base layer proceeds, the base layer becomes more glassy. The diffusivity of solvent in the base layer, and the equilibrium volume fraction of solvent in a swollen layer decrease as the imide fraction increases.[15] These decreases will result in less solvent swelling of the base layer during the spin-casting process. The combination of these kinetic and thermodynamic changes in the solvent swelling of the base layer may reduce the mobility of the dPAE chains into the base layer as the imide fraction increases. Additionally, as the imidization reaction proceeds, the chemical composition of the base layer is changed. Although the PAE and the base layer will eventually convert to the same polyimide, during the spin-casting process they are different polymers with differences in chemical structure, chain stiffness, and mobility. As f increases, an unfavorable enthalpic interaction between the base layer and the precursor will appear and increase.

Neutron reflectometry (NR) was used to profile samples prepared with $f = 0.9$ ($T_i = 300$ °C) and $f = 1$ ($T_i = 400$ °C). This regime is of great interest because the interface was too narrow to be profiled with DSIMS and NRA, yet the G_c changes from ∼30 to ∼700 J/m^2 over this range of imide fraction. Samples were produced with $f = 0.9$ and $f = 1$, and they were analyzed with NR before and after a 400 °C anneal. In this way we investigated the composition profile both after the spin-casting process and after the annealing process. The top PAE layer converts completely to polyimide during the anneal.

Parts a and b of Figure 6 show reflectivity, R, for a sample with $T_i = 300$ °C and $f = 0.9$, where the layers were spun cast from NMP. The data are shown as Rk^4 vs k, where $k = k_{z,i}$. Figure 6a shows the data taken after the second layer was spun cast and dried at 80 °C. The solid line is a simulated fit to the data obtained using the interfacial profile shown in the inset. The best fit to the data was obtained with an interfacial width of 20 ± 10 Å and with a low volume fraction tail of PAE penetrating the base layer for a distance of ∼100 Å, as shown in the inset. The exact shape of the tail may differ from that shown, since R is dominated by the sharp interface. However, there is no question that such a tail exists. Figure 6b shows the data collected after the bilayer sample was annealed at 400 °C for 1 h. The interface broadens to 70 ± 10 Å, and the tail is still present in approximately the same volume fraction.

Figure 7 shows reflectivity data for a sample with base layer $f = 1$, after $T_i = 400$ °C, where the layers

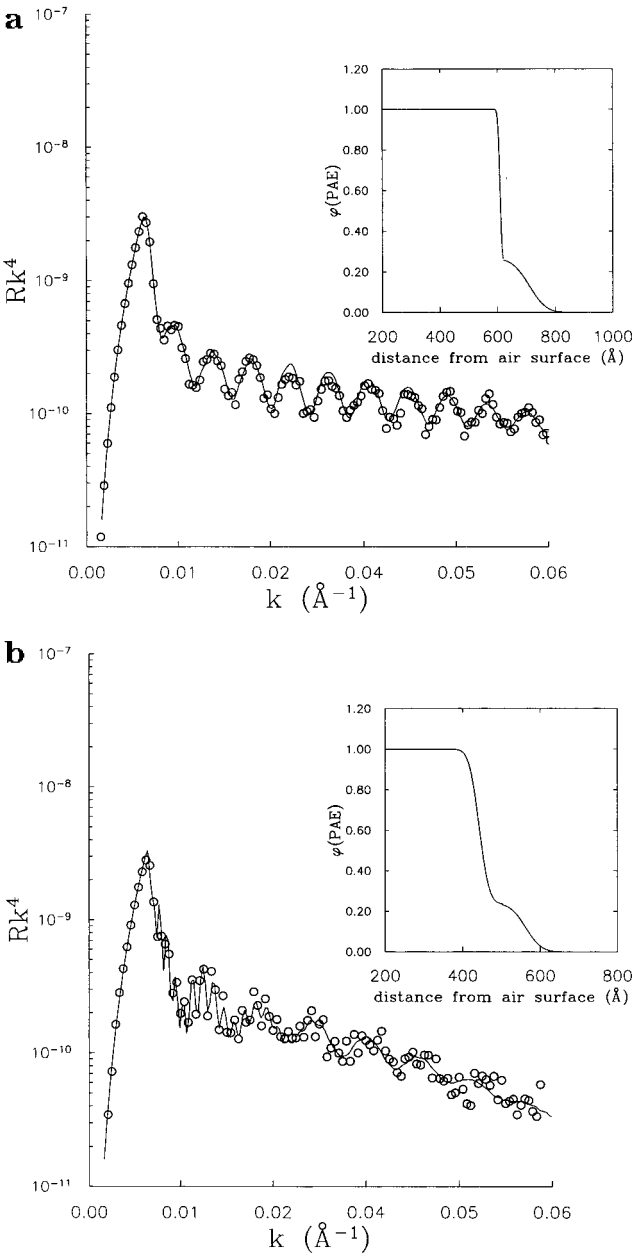

Figure 6. Neutron reflection data (plotted as Rk^4 vs k) of PMDA−ODA bilayers spun cast from solutions of m-PAE in NMP. (a) shows the data after the second layer was spun cast and dried at 80 °C. (b) shows the data after the bilayer was annealed at 400 °C. The solid line is a simulated fit to the data using the interfacial profile shown in the inset. The data were taken at NIST.

were spun cast from NMP. The data shown were collected after the 400 °C anneal. The inset shows the ϕ_{PAE} profile which best fits these data. Use of an error function to model the interface results in a very good fit to the data. There does not appear to be a tail of PAE penetrating the base layer. A sample analyzed after the second layer is deposited before any further annealing had an interfacial width of 25 ± 10 Å. After the bilayer sample is annealed at 400 °C for 1 h, the interface is still well fit using a simple error function and the interfacial width is 33 ± 10 Å.

NR was also used to examine samples spun cast from DMSO. In this case, we found that samples with $T_i =$ 300 and 400 °C had an interfacial width of ∼90 Å after the 400 °C anneal. The sample spun cast from DMSO onto the fully imidized base layer ($T_i = 400$ °C) had an interface substantially broader than a sample cast from

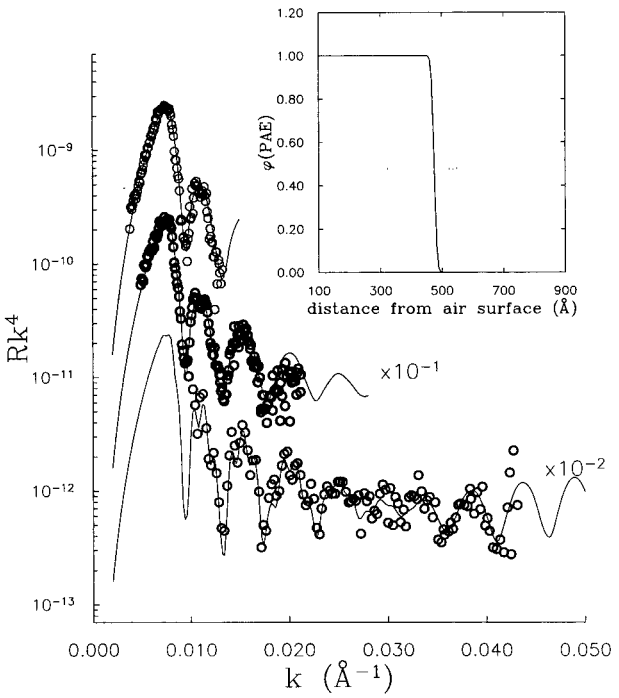

Figure 7. Neutron reflection data plotted as Rk^4 vs k for a PMDA−ODA polyimide bilayer sample spun cast from solutions of *m*-PAE in NMP. The base layer imidization temperature was $T_i = 400$ °C. The solid line is a simulated fit to the data using the interfacial profile shown in the inset. The data were taken at ANL-IPNS. The data were collected at $\theta = 0.5$, 0.7, and 1.4°. On the figure the data for each angle were offset by a factor of 10.

NMP processed in a similar manner. In the case of DMSO, the interfacial width was 88 Å, whereas for NMP, the interfacial width was 25 Å. The origin of this difference is not known at present. The spin-casting solvents swell the polyimide base layer to comparable equilibrium volume fractions with approximately one molecule of solvent absorbed per two repeating units of the PMDA−ODA structure.[16,17] However, the velocity of the case II front differs by about 1 order of magnitude between the two solvents with a DMSO front velocity of $\sim 2 \times 10^{-7}$ cm/s and an NMP front velocity $\sim 2 \times 10^{-8}$ cm/s. Another contributing factor may be that the complexation of the NMP solvent with the PAE polymer which occurs in solution effectively made[18] the chain bulkier and consequently less mobile in the base layer. Such a complexation does not occur with DMSO. An additional possibility is that the ordering and crystallization processes which occur at elevated temperatures were affected by the choice of spin-casting solvent. A denser or more ordered base layer would have less free volume and would also likely have lower solvent absorption rates. A more ordered base layer thus could result in less penetration of the base layer by the spun-on layer, and hence the interface would be sharper.

From this NR study we may surmise that for the *m*-PAE precursors of PMDA−4,4′-ODA spun cast from NMP, the interfacial width is primarily determined during the spin-casting/drying process where interdiffusion is facilitated by the solvent. The interface produced can be very sharp and depends upon the imide fraction of the base layer and the solvent. Even though the differences between the two layers are small, little interdiffusion occurs upon annealing due to the high glass transition temperature (T_g) of PMDA−ODA. A summary of the NR results for the PMDA−ODA bilayers can be found in Table 1.

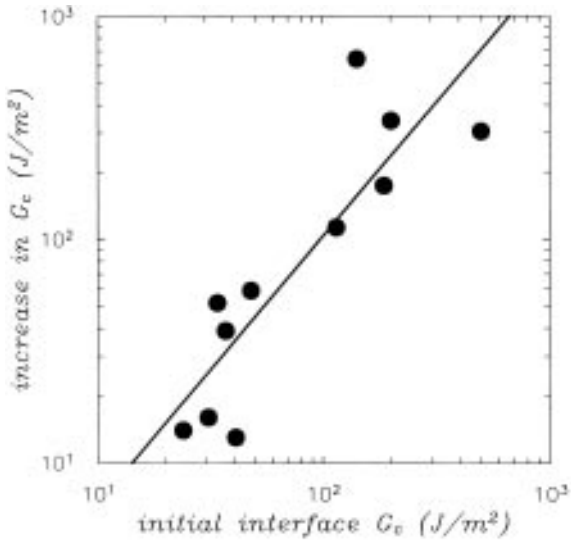

Figure 8. Interfacial fracture energy for samples prepared via the base layer swelling method. The resultant G_c is plotted against the value attained when the base layer is not swollen with solvent. The range of values demonstrates the sensitivity of G_c to base layer imidization conditions. It appears that a 60% increase is attained with the solvent swelling process.

Table 1. Summary of the Neutron Reflection Results for PMDA−ODA Bilayers

T_i (°C)	T_{ann} (°C)	casting solvent	interfacial width d (Å)	ϕ_{PAE} in base layer
300	80	NMP	20 ± 10	0.25
300	400	NMP	80 ± 10	0.25
400	80	NMP	25 ± 10	0
400	400	NMP	33 ± 10	0
300	80	DMSO	75 ± 10	0
300	400	DMSO	88 ± 10	0
400	80	DMSO	88 ± 10	0
400	400	DMSO	98 ± 10	0

The *m*-poly(amic acid ethyl ester) precursor of PMDA−4,4′-ODA, imidized in a stepwise fashion has a broad T_g centered around 400 °C,[13] as measured by Czornyj et al. using dynamic mechanical thermal analysis. It is important to note that at T_g the storage modulus drops only 1 order of magnitude and that PMDA−4,4′-ODA has an E' of $\sim 2 \times 10^8$ Pa when it is above the "glass transition temperature".[13] This result indicates that there is not a high degree of chain mobility even above the T_g, probably due to the competing process of molecular ordering that occurs at these elevated temperatures.[19] Since the 400 °C annealing temperature is not significantly above T_g, it is not surprising that substantial interdiffusion does not occur after a 1 h anneal.

Solvent-Assisted Diffusion. Several researchers have shown that solvent swelling of the polyimide base layer before spin casting the second layer can be an effective means of improving G_c.[2,3] We did a series of *T*-peel measurements and found that the absolute value of strengthening achieved as a result of soaking a base layer in solvent for 1 h depended strongly on the base layer imidization conditions. Our experimental data are plotted in Figure 8. This figure shows that G_c increased ~60% for solvent-swollen samples over samples made in a similar fashion that had not been swollen with solvent before deposition of the second layer.

DSIMS was used in an effort to determine the interfacial changes associated with this process. We anticipated that the interface between the two layers might be substantially broader because the swollen base

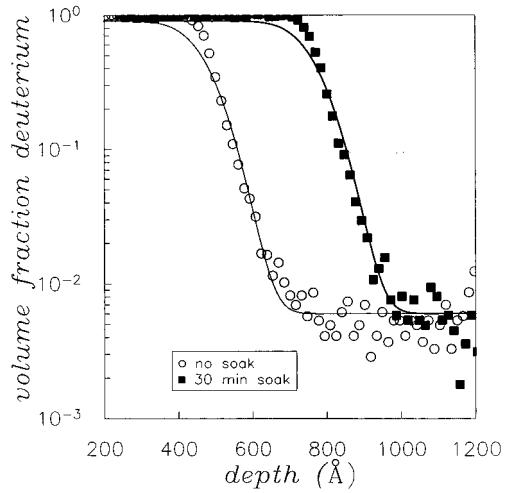

Figure 9. DSIMS profiles of PMDA−ODA interfaces created by swelling the fully imidized base layer (T_i = 400 °C) with NMP for 30 min before deposition of the second layer. There is no broadening of the interface apparent nor is there any enhanced miscibility of the PAE and PI layers.

layer is more easily penetrated by the precursor chains. Fully cured base layers were soaked in NMP for 30 min before spin casting the second layer. This period of time should have been sufficient to fully saturate the ~2000 Å thick base layer with solvent. Figure 9 shows deuterium profiles obtained with DSIMS for the interface between two layers of PMDA−ODA. There is no apparent difference in the width of the interface nor is there any enhanced solubility as a result of the swelling process.

Thermoplastic Polyimides Diffusing into PMDA−ODA. Effect of Annealing Temperature. The case of a thermoplastic polyimide penetrating a glassy polyimide was investigated using layers of ODPA−4,4′-ODA (with a T_g when fully imidized of 270 °C) spun cast onto fully imidized base layers (T_i = 400 °C) of deuterium-labeled PMDA−4,4′-ODA. We used neutron reflectivity to investigate the interfacial profiles as a function of the molecular weight of the ODPA−ODA polymer and as a function of the annealing temperature T_{ann}. Figure 10 shows the neutron reflectivity data for a sample annealed at T_{ann} = 450 °C. This temperatures is well above the glass transition temperature of the ODPA−ODA. The compositional profile that corresponded to a best fit of the neutron reflectivity data is shown in the inset. Figure 10a shows the best fit to the data obtained using a simple error function. The critical k_c is determined by the b/V of the deuterium-labeled PMDA−ODA. In these samples k_c was the same for all the annealing temperatures (80, 350, 400, and 450 °C) and matched the value of a single layer of deuterium-labeled PMDA−ODA polyimide. The value of b/V for the ODPA−ODA layer was determined from a separate single layer sample of ODPA−ODA. It was found that the amplitude of the interference fringes decreased as the annealing temperature increased, indicating a decrease in the difference in scattering length density across the interface. The persistence of the interference fringes to high values of k indicates that the interface is sharp and has not broadened with the higher annealing temperatures. Additionally, Rk^4 asymptotes to a constant value rather than continually decreasing which also indicates that the interface is sharp. The combination of these parameters led us to simulate the data with a reduced $\Delta(b/V)$ at the interface by including a tail of

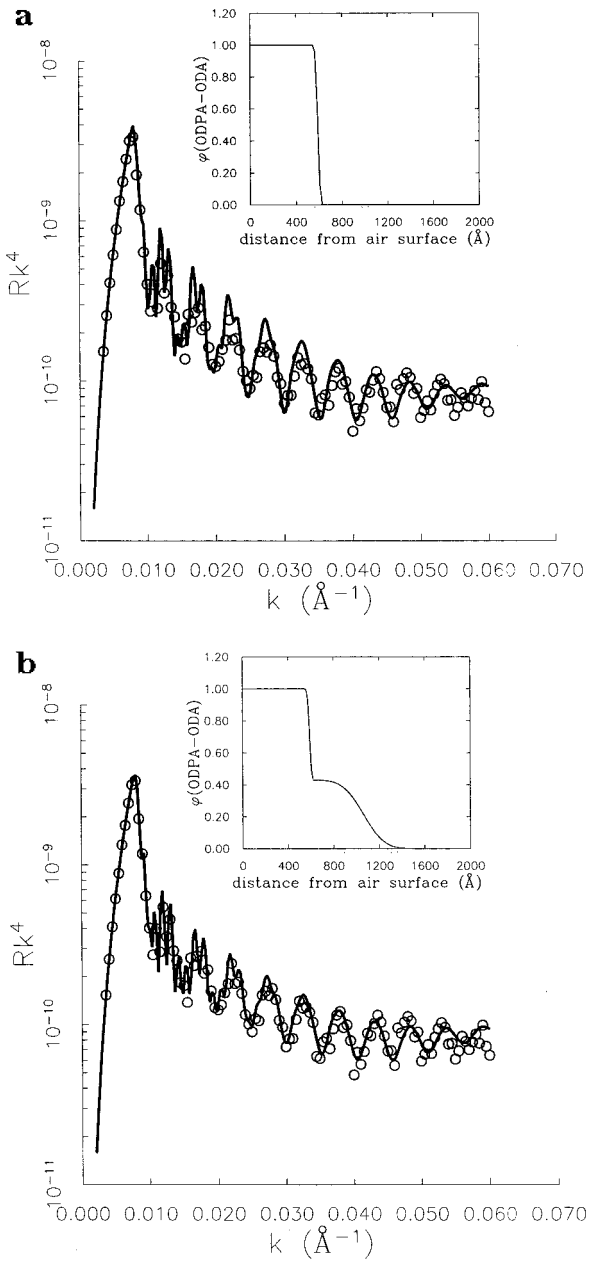

Figure 10. Neutron reflection data (plotted as Rk^4 vs k) of ODPA−ODA spun cast onto fully imidized PMDA−ODA after a 1 h anneal at 450 °C. (a) shows the data fit with a simulated composition profile corresponding to the simple error function shown in the inset. (b) shows a fit to the same data where the interface was simulated with a tail of ODPA−ODA penetrating the PMDA−ODA layer. This simulation is a better fit to the data. The data were taken at NIST.

ODPA−ODA in the deuterium-labeled base layer.[20] Figure 10b shows that a good fit to the data can be obtained by assuming that the ODPA−ODA layer swells the PMDA−ODA layer, as shown in the inset.

Figure 11 shows the composition profiles determined for fitting neutron reflectivity data after a 1 h anneal at (a) 80 °C, (b) 350 °C, (c) 400 °C, and (d) 450 °C. The unannealed sample has an interfacial width of 38 Å. The annealed sample interfaces are only slightly broader than the unannealed sample with interfacial widths of 60 Å for T_{ann} = 350 °C and 50 Å for T_{ann} = 400 and 450 °C samples. As the annealing temperature rises, it appears that the solubility of ODPA−ODA in the PMDA−ODA base layer increases, which causes a tail in the concentration of the ODPA−ODA into the PMDA−

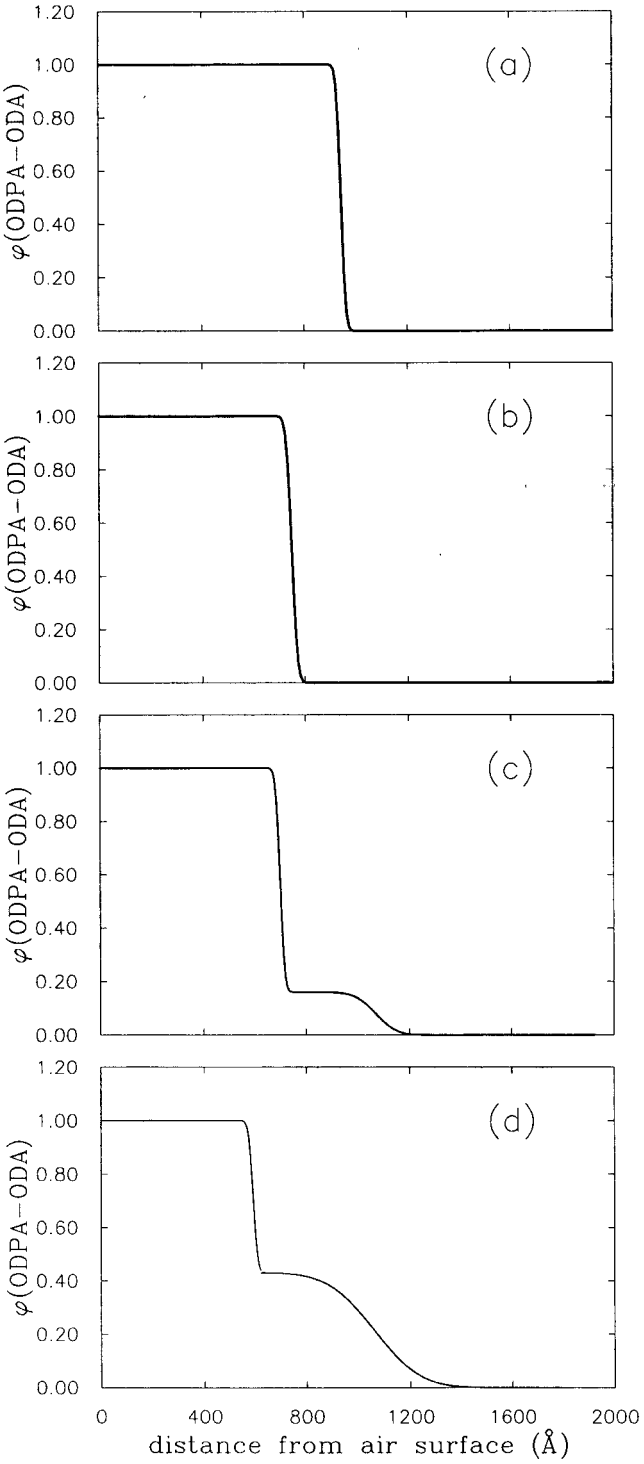

Figure 11. Composition profiles are shown for the ODPA−ODA (M_w = 27k)/PMDA−ODA interface for different annealing temperatures: (a) T_{ann} = 80 °C; (b) T_{ann} = 350 °C; (c) T_{ann} = 400 °C; (d) T_{ann} = 450 °C.

ODA to develop. The depth of penetration cannot be easily determined using NR because this technique is sensitive to sharp changes rather than diffuse changes in scattering length density; however, we know that the tail has not penetrated the entire width of the layer. Since the penetration increases from 400 and 450 °C, the swelling could be limited either by the kinetics or the thermodynamics of the process. It is possible that at low temperatures the two polymers are immiscible and that there is limited solubility at high temperatures.

Another possible explanation for the change in the reflectivity profile is that a transimidization reaction has

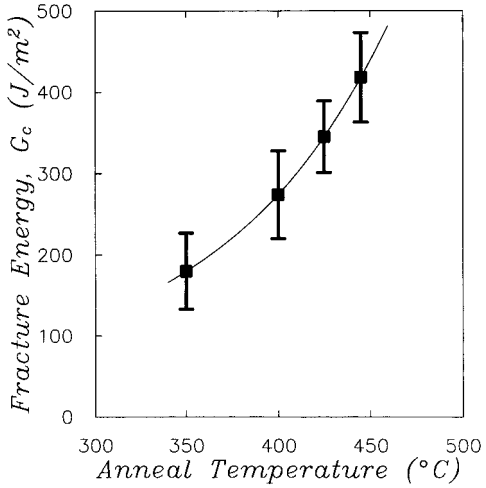

Figure 12. Effect of annealing temperature on G_c for samples consisting of sequentially spun layers of PMDA−ODA, ODPA−ODA (~1500 Å thick), and PMDA−ODA. These films were fully imidized after each film was deposited by spin casting.

occurred at 400 and 450 °C. There is evidence that this reaction occurs for some polymers when raised substantially above their glass transition temperature.[21] In this scenario a reaction occurs at the interface and adjacent d-labeled and protonated polyimide chains exchange segments resulting in the joining of unlabeled and deuterium-labeled chain segments in the same chain. Hence the jump in scattering length density very close to the interface would decrease but in this situation the interface would probably look more symmetric than the profiles shown in Figure 11. Due to the lack of phase information in NR, it is difficult to tell the difference between these two options.

Measurements of G_c verify that the interface strengthens as the annealing temperature increases from 350 °C, as shown in Figure 12. These values support the idea that there are significant changes that occur in the interfacial structure between 350 and 450 °C.

In order to investigate the possibility of enhanced miscibility between the polymers at elevated temperatures, mixtures of the poly(amic acid) of ODPA−ODA and the *m*-poly(amic acid ethyl ester) of PMDA−ODA were prepared in solution. The use of a PAA and a PAE precursor prevented monomer exchange in solution.[22] The solutions were prepared with a ratio by weight of 1:1, 1:3, and 1:4, dropped onto glass slides, and allowed to dry in an oven. The films were examined optically with an interference microscope. All of the solutions were clear. The films prepared from the 1:1 and 1:3 blends were cloudy. There was strong phase separation apparent both after drying and after annealing the film at 450 °C for 4 h. Phase separation in the cast film can occur as a result of both the different monomeric compositions of the two polyimides and the differences between the poly(amic acid) and the poly(amic acid ethyl ester).[23] In contrast a 1:4 blend showed no apparent phase separation in either the cast or the annealed film. These results suggest that ODPA−ODA polyimide may be soluble to a limited degree in PMDA−ODA.

This experiment gives support to the notion that NR detected penetration of the ODPA−ODA into the PMDA−ODA after the high-temperature anneals. For a 450 °C anneal, both the PMDA−ODA and the ODPA−ODA material are above their glass transition temperatures. However, the ODPA−ODA chains have much greater mobility than the PMDA−ODA chains due to

Table 2. Results of Neutron Reflection Analysis of ODPA−ODA/PMDA−ODA Interfaces[a]

M_w	interfacial width (Å)
27k	60
64k	60
190k	55

[a] The value in the table is the interfacial width after a 1 h anneal at $T_{ann} = 350$ °C for a variety of molecular weight ODPA−ODA polymers.

their greater flexibility and amorphous character. Ordering processes occur at the high temperature which restrict the mobility of the PMDA−ODA chains even above their T_g. The PMDA−ODA acts like a gel network where the ordered regions act like cross-links and allow a limited amount of penetration. Hence there is not sufficient mobility for the PMDA−ODA chains to diffuse significant distances, but there is sufficient mobility of the PMDA−ODA molecules to allow them to be swollen by the ODPA−ODA chains. The shape of the composition profiles can be explained by a much higher diffusivity of the ODPA−ODA as compared to the PMDA−ODA chains.

Similarly shaped composition profiles were seen by Hobbs et al. for the diffusion bonding of poly(butylene terephthalate) (PBT) to BPA polycarbonate (BPAPC).[24] PBT has a $T_g = 45$ °C, and BPAPC has a $T_g = 150$ °C. They found that if they annealed the samples above 150 °C, diffusion bonding occurred. However, the interface formed was asymmetric, and the lower T_g PBT polymer swelled the BPAPC. The solubility of the PBT in the BPAPC was a function of temperature. Regardless of the diffusion time involved, the G_c was limited by annealing temperature. This result implies that the G_c of the interface was limited by the number of interface crossings rather than by the depth of the diffusion of the BPT. No diffusion of BPAPC into the PBT was observed.

Another group of researchers, Fernandez et al., used neutron reflectometry to investigate the interface between solution-chlorinated polyethylene (SCPE) and deuterated poly(methyl methacrylate) (dPMMA) as a function of annealing time above T_g.[25] They also found that the profiles could not be fit by simple Gaussian or linear profiles. They attributed the composition profile to the swelling of the less mobile species by the more mobile one.

Effect of ODPA−ODA Molecular Weight. The effect of the molecular weight of the ODPA−ODA on the interfacial profile was examined, and the results are shown in Table 2. The experimental data could be fit with an error function and the profile across the interface appeared to be symmetric. The molecular weight does not affect the width of the interface formed after spin casting and annealing at $T_{ann} = 350$ °C.

Solvent-Assisted Diffusion of Thermoplastic Polyimides. A deuterium-labeled fully imidized PMDA−ODA layer was soaked with solvent (either NMP or methylene chloride) for 40 min, and then the surface was covered with a solution of the poly(amic acid) of ODPA−ODA. This was allowed to sit on the surface for 3 min before spinning, following which the sample was annealed at 400 °C. The swelling of the PMDA−ODA would enhance mobility and dilute the contacts between the chemically different PMDA−ODA and ODPA−ODA materials. We used both NMP and CH_2Cl_2 to swell the base layer because of the differences in their absorption behavior. Case II type diffusion is observed for both polymer−penetrant systems. The ratio of the number of absorbed solvent molecules to polymer repeat units is ∼1:2 for both NMP and CH_2Cl_2 solvents.[17,26] The case II solvent front velocity is about 2 orders of magnitude higher for the CH_2Cl_2 ($v \sim 7 \times 10^{-6}$ cm/s)[26] than for the NMP ($v \sim 2 \times 10^{-8}$ cm/s).[17] The results of these experiments are shown in Table 3. The interface does not broaden significantly for either the NMR- or the CH_2Cl_2-soaked samples. However the slight increase may be sufficient to explain the corresponding increase in G_c. The narrow interfaces which result suggest that the interfacial width is not primarily driven by the kinetics of solvent diffusion.

Table 3. Results of a Neutron Reflection Analysis of Solvent Swelling on the Interfacial Width of ODPA−ODA/PMDA−ODA Samples

swelling solvent	interfacial width (Å)
none	50 ± 10
NMP	55 ± 10
CH_2Cl_2	60 ± 10

Relationship between G_c and R_g. Blocks of the same polymer or miscible polymers can be welded together by bringing them in contact and annealing above the glass transition temperature (T_g). During the welding process the polymer chains interdiffuse and form entanglements, thus strengthening the interface. The number of effective crossings of the interface and the average interpenetration depth have both been cited as factors that control the strength. In theory, polymer chains need only diffuse a distance comparable to their radius of gyration for the interfacial strength of the sample to return to the bulk value.[27] The radius of gyration (R_g) for the *m*-PAE of PMDA−ODA of $M_w = 40\,000$ is ∼60 Å.[28] According to such estimates, there should then be complete strength recovery for the PMDA−ODA system with diffusion distances slightly less than 60 Å and interfacial widths comparable to $(2\pi)^{1/2}R_g$ or ∼150 Å. As a result, very high resolution depth profiling methods are needed in order to resolve interfaces that have less than the bulk strength. For spun-cast polyimide films, it is not clear if diffusion depths on the order of R_g will be sufficient for maximal stress transfer. The situation is complicated by in-plane orientation of chains, molecular ordering, and segmental stiffness.

Figure 13 is a plot of the G_c values as a function of the diffusion distance obtained from neutron reflection. The figure contains data for both the PMDA−ODA bilayers and the PMDA−ODA/ODPA−ODA/PMDA−ODA trilayer samples. For the PMDA−ODA/ODPA−ODA/PMDA−ODA interfaces, only the $M_w = 27\,000$ ODPA−ODA sample was included with $T_{ann} = 350$ °C because this composition profile was well fit, simulating the interface as an error function. Hence the interfacial width is easily characterized and compared to the values of interfacial width for PMDA−ODA/PMDA−ODA interfaces with $0.9 < f \leq 1.0$ which are also well fit, simulating the interface as an error function. Figure 13 shows that the G_c increased as the diffusion distance w increased. The largest w corresponds to $\sim^{1/2}R_g$. While the G_c had not reached a limiting value, it did increase significantly and the interface was fairly strong for $w \cong {}^{1/2}R_g$.

The data from DSIMS, NRA, and NR combine to give a more detailed picture of the PMDA−ODA interfaces than was available previously. Our data do not agree with the observations of Brown et al.[29] where for the

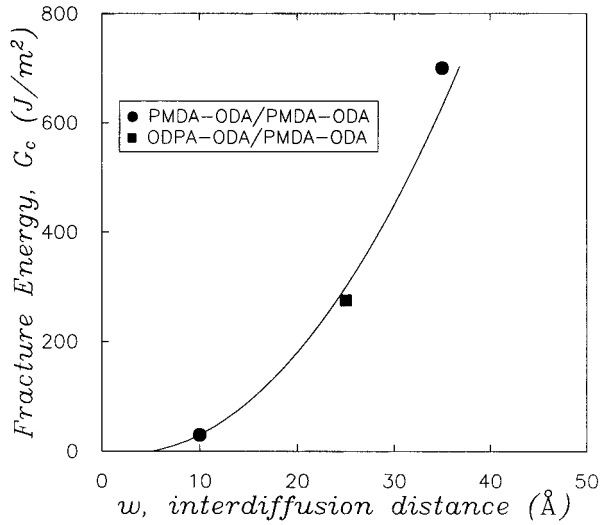

Figure 13. Interfacial fracture energy plotted as a function of the interdiffusion distance. The figure includes data for both the PMDA−ODA/PMDA−ODA and the ODPA−ODA/PMDA−ODA interfaces.

PAA precursors of PMDA−4,4′-ODA, they found that an interdiffusion distance on the range of hundreds of nanometers was required to achieve good adhesion. Our measurements indicate that the interfaces are sharper and have a different shape than this earlier study indicated. The present measurements were made with neutron reflectometry, which has subnanometer resolution and hence provides a more detailed view of the interface than was available with FRES. In our present work we found that the interfaces formed for $f < 0.9$ are asymmetric. There is limited solubility of the PAE chains in the base layer which decreased with the imide fraction of the base layer. The G_c probably depends upon a combination of the bulk mixing observed at the interface, and the solubility of chains in the base layer which gives rise to the tail in the composition profile. Figure 13 shows us that for samples which may be characterized with a simple erfc profile, the width of the interface affects G_c. We have also found that when the width of the steep part of the interface is kept constant, increasing the tail of the asymmetric composition profile will also increase G_c. This fact was demonstrated in Figure 12 for the ODPA−ODA/PMDA−ODA interfaces where an increase in T_{ann} from 350 to 450 °C results in increased solubility of ODPA−ODA in the PMDA−ODA base layer and corresponding increases in G_c from 180 to 420 J/m^2. For the ODPA−ODA/PMDA−ODA interfaces or the PMDA−ODA/PMDA−ODA interfaces, which have composition profiles indicating that chains from the top layer penetrate into the base layer, we believe that there is more than sufficient penetration by the tracer into the bulk of the polymer for entanglements to occur even in a system which has a lot of in-plane chain orientation. However, the limited solubility of PAE chains in the base layer limits the number of chains crossing the interface and hence the G_c.

Summary

The relationship between the interfacial composition profile and the fracture energy was examined for polyimide layers. For bilayers of PMDA−ODA we found that the samples with incomplete base layer imidization did not have the error function profiles expected for solution of Fick's laws. Rather, there was a sharp interface between the dPAE and the base layer with a long, low volume fraction tail of dPAE penetrating into the base layer. This profile is formed during the spin-casting process and does not broaden after annealing at 400 °C. The interface of PMDA−ODA bilayers prepared from NMP solutions with f between 0.9 and 1.0 are well fit using the classical error functions and are very sharp. A sample with $f = 1$ has an interfacial width of ∼30 Å and a sample with $f = 0.9$ has an interfacial width of ∼80 Å.

Interfaces between PMDA−ODA and the thermoplastic polyimide ODPA−ODA were also examined using neutron reflectometry. We found that the initial interface formed during the spin-casting process was slightly broader than that of the PMDA−ODA bilayers. This broadening is likely due to the comparatively greater flexibility and mobility of the ODPA−ODA precursor in solutions. We found that the interface width of the sharp part of the interface after annealing at $T = 350-450$ °C was ∼55 Å. While an increase in the annealing temperature does not cause large scale mixing at the interface, it does appear to allow a low volume fraction of ODPA−ODA chains to diffuse into the PMDA−ODA, effectively swelling the more rigid system. The increased tail of the asymmetric composition profile results in a stronger interface.

Acknowledgment. We gratefully acknowledge the support of the Semiconductor Research Corp. through the Electronic Packaging Program, IBM, and the Cornell Electronic Packaging Alliance. N.C.S. was partly funded by a Department of Education Polymer Fellowship. S. Chandra and J. Lai performed many of the *T*-peel measurements. We acknowledge helpful discussions with L. Matienzo about the solvent swelling experiments. P. Gallagher, W. Orts, J. Van Zanten, and W. Wallace of NIST are gratefully acknowledged for their assistance in the reflectivity measurements. The reflectivity measurements done at Argonne National Laboratory were done with the assistance of W. Dozier. The IPNS facility at Argonne is funded by the U.S. Department of Energy under contract W-31-109-ENG-38. We benefited from the use of the facilities of the Cornell Materials Science Center and from the facilities of the National Nanofabrication Facility at Cornell University, both of which are funded by the NSF.

References and Notes

(1) Stoffel, N. C.; Chandra, N. C.; Kramer, E. J.; Volksen, W.; Russell, T. P. Submitted to *Polymer*.
(2) Brown, H.; Yang, A. C. M. *J. Adhesion Sci. Technol.* **1992**, *6* (3), 333.
(3) Saenger, K. L.; Tong, H. M.; Haynes, R. D. *J. Polym. Sci., Polym. Lett. Ed.* **1989**, *27*, 235.
(4) Stoffel, N. C.; Hsieh, M.; Kramer, E. J.; Volksen, W. *J. Components Packaging Manufacturing, Part B*: *Adv. Packaging*, in press.
(5) Volksen, W.; Yoon, D. Y.; Hedrick, J. L.; Hofer, D. In *Materials Science of High Temperature Polymers for Microelectronics*; Grubb, D. T., Mita, I., Yoon, D. Y., Eds.; MRS Symposium Proceedings Vol. 227; Materials Research Society; Pittsburgh, PA, 1991; p 23.
(6) Stoffel, N. C.; Kramer, E. J.; Volksen, W.; Russell, T. P. *Polymer* **1993**, *34* (21), 4524.
(7) Bower, G. M.; Frost, L. W. *J. Polym. Sci., Part A*: *Polym. Chem.* **1963**, *1*, 3135.
(8) Chaturvedi, U. K.; Steiner, U.; Zak, O.; Krausch, G.; Schatz, G.; Klein, J. *Appl. Phys. Lett.* **1990**, *56*, 1228.
(9) Russell, T. P. *Mater. Sci. Rep.* **1990**, *5*, 179.
(10) Born, M.; Wolf, E. *Principles of Optics*; Pergamon Press: Oxford, U.K., 1975.
(11) Karim, A.; Arendt, B. H.; Goyette, R.; Huang, Y. Y.; Kleb, R.; Felcher, G. P. *Physica B* **1991**, *173*, 17.

(12) Private communication from Keshav Prasad, IBM Corp.
(13) Czornyj, G.; Chen, K. R.; Prada-Silva, G.; Arnold, A.; Souleotis, H.; Kim, S.; Ree, M.; Volksen, W.; Dawson, D.; Di Pietro, R. Polyimide for Thin Film Redistribution on Glass-Ceramic/Copper Multilevel Substrates (ES9000 system). *Proc. Electron. Compon. Technol. Conf., 42nd* **1992**, 682.
(14) Tead, S. F.; Kramer, E. J.; Russell, T. P.; Volksen, W. *Polymer* **1990**, *31*, 520.
(15) Honneker, C. B. S. thesis, Department of Materials Science, Cornell University, 1991.
(16) Unpublished data of N. Stoffel and C.-A. Dai. FRES and RBS were used to study the absorption of d-NMP and DMSO solvent into PMDA−ODA polyimides prepared from *n*-PAE precursors, imidized at 400 °C. The NMP and DMSO show case II type diffusion. The swollen core reaches comparable weight fractions of ∼12% solvent after 10 min at room temperature.
(17) Gattiglia, E.; Russell, T. P. *J. Polym. Sci., Polym. Phys. Ed.* **1989**, *27*, 2131.
(18) Brekner, M.-J.; Feger, C. *J. Polym. Sci., Polym. Chem. Ed.* **1987**, *25*, 2005.
(19) Takahashi, N.; Yoon, D. Y.; Parrish, W. *Macromolecules* **1984**, *17*, 2583.
(20) We also tried simulations with reduced $\Delta(b/V)$ at the polymer−polymer interface by introducing a tail into both the deuterium-labeled and the protonated polyimide layers. However, the simulation did not fit the data as well as the simulation shown in Figure 10b.
(21) Volksen, W. Condensation Polyimides: Synthesis, Solution Behavior and Imidization Characteristics. In *Advances in Polymer Science*; Springer-Verlag; Berlin and Heidelberg, 1994; Vol. 117, p 111.
(22) Ree, M.; Yoon, D. Y.; Volksen, W. *J. Polym. Sci., Part B: Polym. Phys.* **1991**, *29*, 1203.
(23) Saraf, R. F. *Macromolecules* **1993**, *26* (14), 3623.
(24) Hobbs, S. Y.; Watkins, V. H.; Bendler, J. T. *Polymer* **1990**, *31*, 1663.
(25) Fernandez, M. L.; Higgins, J. S.; Penfold, J.; Shackleton, C. *J. Chem. Soc., Faraday Trans.* **1991**, *87* (13), 2055.
(26) Matienzo, L. J.; Emmi, F.; VanHart, D. C.; Lo, J. C. *J. Vac. Sci. Technol.* **1991**, *A9* (3), 1278.
(27) Kausch, H. H.; Tirrell, M. *Ann. Rev. Mater. Sci.* **1989**, *19*, 341.
(28) Cotts, P. *Polym. News* **1990**, *15*, 110.
(29) Brown, H.; Yang, A. C.-M.; Russell, T. P.; Volksen, W.; Kramer, E. J. *Polymer* **1992**, *33*, 3384.

MA9601880